COMBINING FLOOD DAMAGE MITIGATION WITH TIDAL ENERGY GENERATION: LOWERING THE EXPENSE OF STORM SURGE BARRIER COSTS

David R. Basco, Civil and Environmental Engineering Department, Old Dominion University, Norfolk, Virginia, 23528, USA

Storm surge barriers across tidal inlets with navigation gates and tidal-flow gates to mitigate interior flood damage (when closed) and minimize ecological change (when open) are expensive. Daily high velocity tidal flows through the tidal-flow gate openings can drive hydraulic turbines to generate electricity. Money earned by tidal energy generation can be used to help pay for the high costs of storm surge barriers. This paper describes grey, green, and blue design functions for barriers at tidal estuaries. The purpose of this paper is to highlight all three functions of a storm surge barrier and their necessary tradeoffs in design when facing the unknown future of rising seas.

INTRODUCTION

Accelerating sea levels are impacting the over 600 million people worldwide currently living near tidal estuaries in coastal regions. Residential property, public infrastructure, the economy, ports and navigation interests, and the ecosystem are at risk. Climate change has resulted from the burning of fossil fuels (oil, coal, gas, gasoline, etc.) and is the major reason for rising seas. As a result, conversion to renewable energy sources (solar, wind, wave, and tide.) is taking place. However, tidal energy is the only renewable energy resource that is available 24/7 with no downtime due to no sun or no wind or no waves. The daily tidal variation at the entrance to tidal estuaries is always present and is the driving force for the resulting ecology and water quality. But the connection to the ocean permits elevated water levels from storm events to penetrate inland causing inundation and flood damage. And that is the problem which will only get worse in the future.

Definition of a Storm Surge Barrier

The barrier at tidal estuaries has come to be called a "storm surge barrier" because the original function was to reduce the elevated water levels during coastal storms and mitigate storm damage. Figure 1 schematically displays the three main section types of a storm surge barrier, namely: the fixed, flood wall sections; the movable, tidal-flow gate sections; and the navigation channel, sector-gate section. Both types of gates are closed during storm events. In some cases, a navigation lock may be present for ship passage during storm events when the gates are closed.
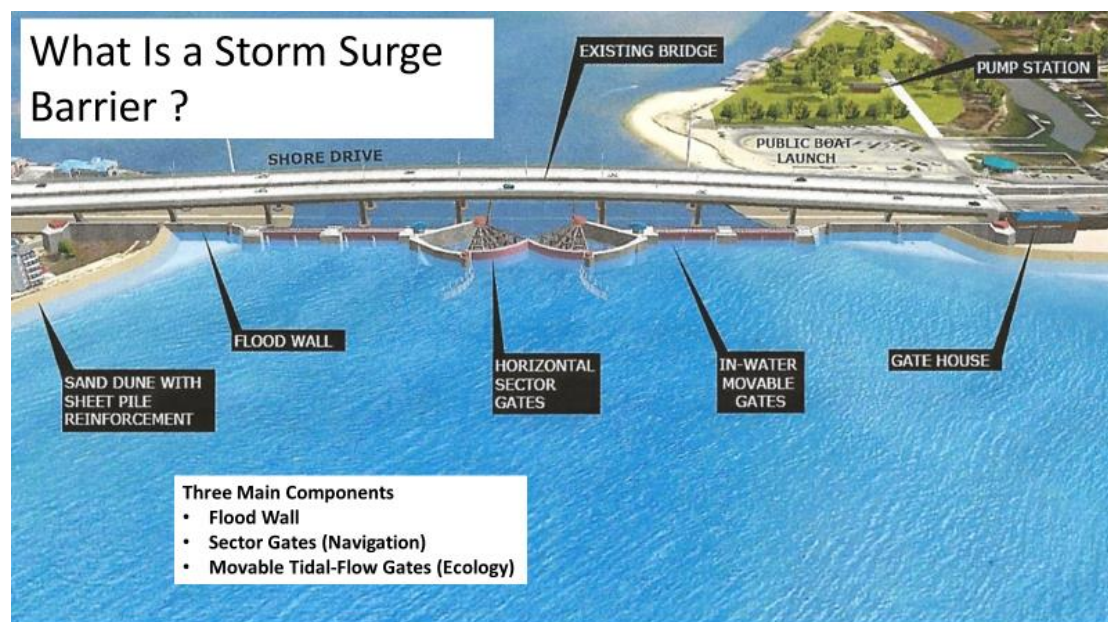

Figure 1. Schematic plan view of the three elements of a storm surge barrier (Lynnhaven Inlet, Virginia Beach, VA).

Grey, Green, and Blue (Tribrid) Design

Barriers across tidal inlets can be designed to reduce inundation and storm surge flooding (grey function), to include normally open, tidal-flow gates to retain ecological resilience (green function), and to incorporate tidal-flow turbines in the gate openings to generate renewable energy (blue function). The combined design to reduce flood damage, maintain the estuary ecology, and generate electrical power requires tradeoffs in the design. The number of solid-barrier sections and gate-opening sections, and magnitude of the flood flowrates through the gate openings are all interdependent quantities that influence the design.

We herein consider a true tribrid design having three distinct, individual components as schematically illustrated in Figure 2. All three functions (grey, green and blue) must work both today and in the distant future of climate change where seas will be much higher and coastal storms more frequent and intense. The grey function to mitigate storm damage, the green function to maintain the estuarine ecology, and the blue function to generate renewable energy (to replace fossil fuel generated energy) will become ever more valuable for citizens of the future living along the worlds coasts.
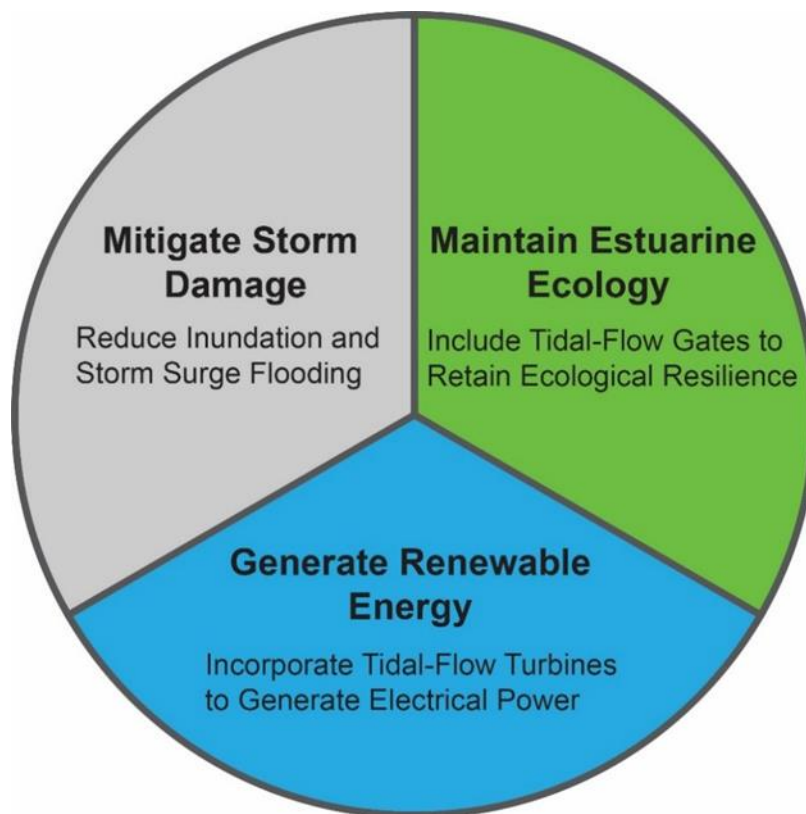

Figure 2 Schematic of Grey, Green and Blue design criteria for three functions of storm surge barriers.

TIDAL ESTUARY ECOLOGY (Green Function)

Hydrodynamics of Daily Tidal Flows

Three dimensional, numerical models are now routinely employed to simulate both hydrodynamic, and estuarine mass transport processes necessary to quantify water quality and ecological change. However, consider here a one-dimensional slice as illustrated in Figure 3 to focus on the upstream limit of the daily high-water tidal level. The tidal amplitude at the entrance to the tidal estuary is the external forcing function and from there the unique shape, water depths, boundary conditions (bottom roughness, end reflections, length of estuary) and mixing modify the propagating tidal amplitude in some complicated way. Figure 3 illustrates this as a decaying, dotted blue line to reach the upstream, present-day limit of the high tide. Tidal "attenuation" is the vertical distance between high water, tidal amplitude at the entrance and the elevation/location where this amplitude is zero.
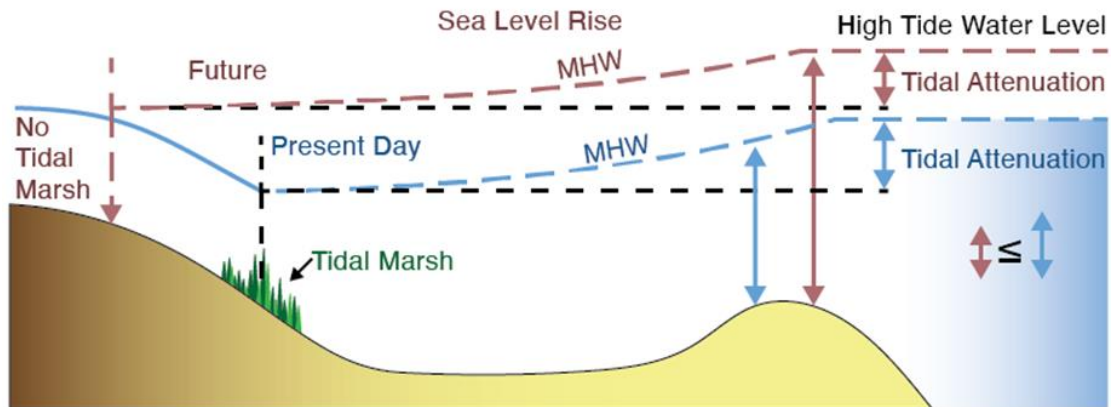
Estuaries

Figure 3. Schematic of location of the present-day (blue) and future (red) upstream limit for high tide water levels.
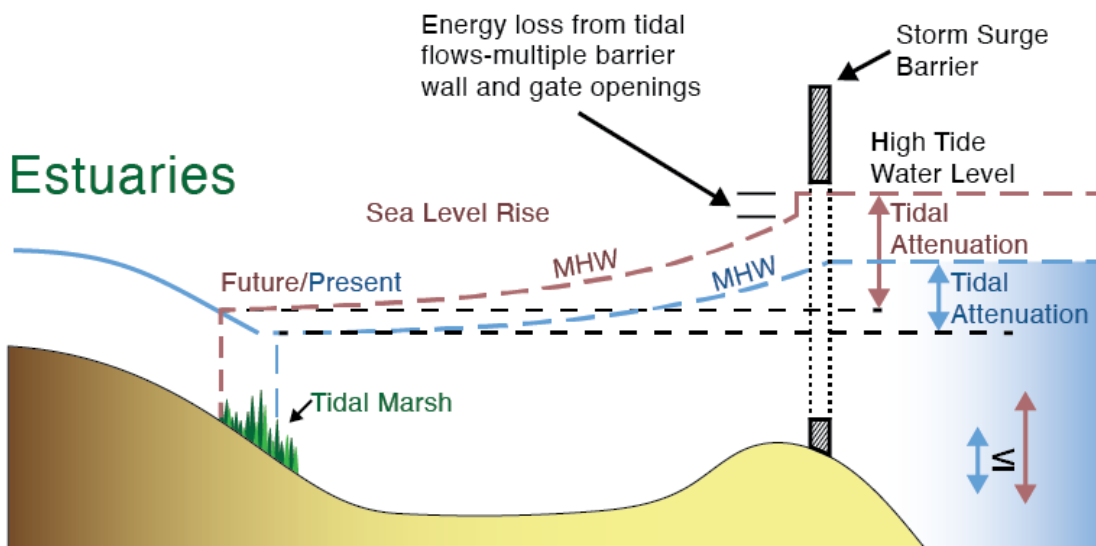

Figure 4. Schematic of location of the present-day (blue) and future (red) upstream limit for high tidal water levels incorporating floodplain alternations that significantly increase tidal energy dissipation. The future upstream limit is near today's location to preserve today's ecology and tidal marsh locations.

Water Quality and Ecology

Saltwater marsh areas around the fringes are the tidal wetlands within the intertidal zone. As shown in Figure 3, today's tidal wetlands lie between the high tide, zero water level location (blue dotted line reaches zero) and the low, tidal levels further seaward at this boundary. Rapid increase in water depth may result in the loss of tidal wetlands which become "drowned" when no longer exposed to the daily fluctuations of the high- and low-tidal cycle. This is also illustrated schematically in Figure 3. Even with the decrease in tidal energy dissipation due to increase water depths (red dotted line reaches zero) the future location of the intertidal zone may not be able to move fast enough to this upland location to maintain a tidal wetland marsh. The result is loss of tidal wetlands due to sea level rise.

Positive Impact of Storm Surge Barriers Under Future Sea Level Rise

As future sea levels increase, the key to maintaining today's water quality and the ecology of tidal wetlands is to significantly increase tidal energy dissipation (Khojasteh et al., 2020). The positive impact of storm surge barriers is the additional increase in tidal energy dissipation at the barrier gates that is necessary to keep the limit of high tide water levels at today's location as illustrated in Figure 4. As sea levels increase, the energy loss should also increase so that the future tidal range below MHW is located at or near the present location. Resilience of the tidal marshes within the estuary will be the

result. This energy loss increase may be achieved by forcing daily tidal flows through fewer tidal-flow gate opening in the barrier. When future storm surges occur that require tidal-flow gate closure, some gates can remain closed after the storm to create more energy loss during normal tidal flow conditions.

The negative perception of storm surge barriers on water quality and the ecology of tidal estuaries must be changed. Under future, much higher sea levels, the goal will be to maximize the energy loss past the open gates to retain the tidal wetlands that exist today.

TIDAL ENERGY PRODUCTION (Blue Function)

Types of Tidal Energy

There are two distinct types of barriers across tidal inlets to capture the daily energy of the tide. One type is the tidal barrage which is similar to a dam with sluice and turbine for generation of hydropower. A potential energy (head differential) is converted to flow velocity through the turbine to generate power.

In contrast, tidal-stream turbines (TSTs) convert the kinetic energy of the tidal flows directly to electrical energy and do not require impoundment of water levels for potential energy. Storm surge barriers across tidal estuary inlets are not tidal barrages because they are not designed to impound water to create a potential energy (head differential). They are called "hydrokinetic" energy turbines that produce tidal-streaming energy.

Tidal Streaming Energy

Two types of tidal-streaming turbines are shown in Figure 5. The left side photo is one unit as designed by Ocean Renewable Power Co (ORPC) called TidGen™. Multiple units can be combined with one power takeoff system and the blades rotate in opposite directions when velocities come from the flood and ebb flow directions. The low profile of the unit permits operation in shallow water.

On the right side in Figure 5 is a horizontal-axis tidal turbine graphic depicting the terminology as borrowed from the wind turbine industry. Verdant Power, Inc. manufactures the Gen5™ Free Flow System unit in the US. The entire unit must be rotated 180º to always be facing directly into the flood or ebb flow directions.

Design of horizontal-axis, water-flow turbines has benefitted from many years of research, testing and field experience for wind turbines. Rotation speed, ω (radians/second) is low (< 10 rad/sec) with few blades (2-3) in both wind and water turbines. The vast difference in fluid density, ρ (water is 800 times denser than air) permits the diameter of the outer tip of the rotor blades, D for water turbines to be far smaller than wind turbines.
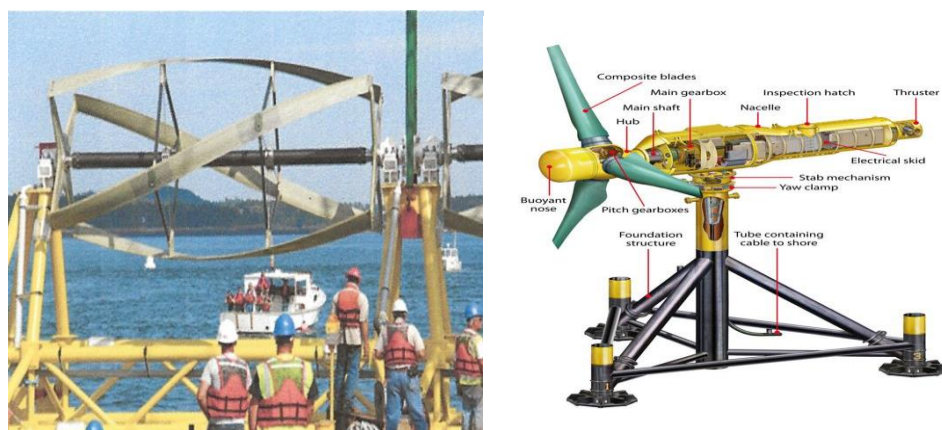

Figure 5. Left-side photo of TidGen™ Power System of Ocean Renewable Power Co. (ORPC) and right-side graphic of Gen5™ Free Flow System of Verdant Power, Inc.

Power Output Curves

Turbine efficiency in power generation is called the "power coefficient", C_p defined as

$$C_p = \frac{Electrical\ Power\ Output\ from\ Turbine}{Water\ Power\ Input\ from\ Velocity} = \frac{P}{\left(\frac{1}{2}\right)\rho A V^3} \tag{1}$$

with $A = \pi R^2$, the flow area for a horizontal turbine with radius, R = D/2

ρ = the mass density of the water

and V = the water velocity moving past the horizontal turbine.

The denominator in Equation (1) is simply the kinetic energy of water velocity (1/2 ρV^2) passing through the projected area, A with velocity, V.

Solving for the power output from the turbine, P gives

$$P = (1/2)\ \rho\ A\ C_p\ V^3 \tag{2}$$

The power output, P of the tidal-flow turbine is also simply the torque, T times the rotational speed, ω.

$$P = T\ \omega \tag{3}$$

and is a function of the rotor blade diameter, D, rotating at speed, ω, fluid density, ρ, dynamic viscosity, μ, and water velocity, V flowing past the turbine.

Rotational speed, ω of the rotor for a given turbine size (blade diameter, shape, number) and given mass density of materials used to manufacture the turbine, depends on the water velocity, V flowing past the turbine. The shape of the blade is patterned after airfoils that produce variable lift and drag forces along the blade which then produce the blade torque, T (lift force x radius). The combination of lift and drag at some angle of attack will produce the maximum combination of lift and drag and largest torque. Clearly, for hydrofoils that vary in shape from the hub to the tip, the total torque produced is also variable along the blade. As a result, the non-dimensional, tip-speed ratio, λ (or TSR) defined as

$$\lambda = \frac{Angular\ velocity\ of\ tip\ of\ blade}{Free-stream\ veloity} = \frac{\omega R}{V} \tag{4}$$

(where R= D/2, the radius to the outer tip of the rotor blade) has been found useful to correlate the measured torque from physical models in the laboratory and calculated torque from computational fluid dynamics (CFD) models.
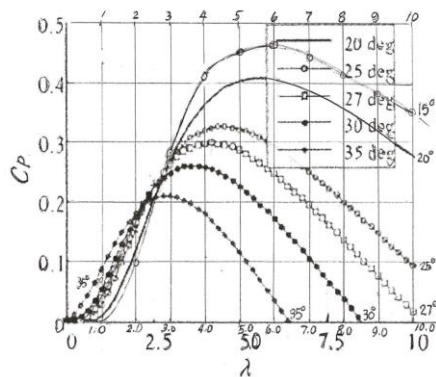

Figure 6 Generic, power generation coefficient as function of tip-speed ratio and blade pitch angle (from Khan, 2018)

Figure 6 (from Khan, 2018) then displays the relation between the turbine efficiency as measured by the power coefficient, C_p on the vertical axis and the tip speed ratio, λ on the horizontal axis for use

5

in estimating the turbine power output, P from Equation (2). The second independent variable is the blade pitch angel, θ which may vary between 15 to 35 degrees. Clearly, the goal in tidal-flow turbine design is to provide tidal-flow velocity, V through the tidal-flow gates to maintain tip-speed rations in the 4-7 range to keep the power coefficients as high as possible. The theoretical maximum value of C_p is the Betz Limit (0.59)

US Potential for Tidal Power Generation at Natural Sites

As of this writing, the United States, Department of Energy (DOE) and their Office of Energy Efficiency and Renewable Energy (EERE) within the Water Power Technology Office (WPTO) only has considered the generation of tidal power at natural sites. Kilcher et al. (2016) presented a ranking methodology for US sites using six criteria (tidal power density, market size, avoided energy cost in the market, distance from site to power grid, shipping cost for construction, and water depth).

Tidal-flow turbines have been generating electricity just north of the Roosevelt Island bridge in the East River between Manhattan and Queens, NYC since 2006. Between 2006-2009, six, Gen4 turbines (D = 4m, 2 blades) delivered over 9,000 turbine-hours of operation. The nominal power rating for each Gen5 turbine (D = 5m, 3 blades) is 35kW. The 10-yr goal is to have 30 turbines (3 tri-mounted on 10 foundations) to generate 1 MW of electrical power.

Positive Impact of SSB Under Future SLR

The Department of Energy's Office of Energy Efficiency and Renewable Energy (EERE) published the report "*Powering the Blue Economy: Exploring Opportunities for Marine Renewable Energy in Maritime Markets*"(April, 2019). Chapter 8 was entitled "Coastal Resiliency and Disaster Recovery" where a key finding was:

"*Shoreline protection and defense of coastal environments is a growing necessity in the face of sea level rise and more intense storms. The development of breakwaters, berms, groins, storm surge barriers, and other similar coastal structures will increase globally, presenting the opportunity for the integration of marine energy devices… providing the dual benefit of shoreline protection and power generation*" (p 99-100).

The Eastern Scheldt storm surge barrier (Holland) has operated five tidal-flow turbines within one gate opening to generate electricity since 2015. This is an ongoing research area entitled "Blue Barriers" at the Tidal Technology Center, Grevelingendam, the Netherlands.

STORM DAMAGE MITIGATION (Grey Function)

Primary Function

Numerical models of the daily tidal amplitudes and currents in three space dimensions and time are now routinely applied to simulate local tidal conditions anywhere in the tidal estuary. (e.g. ADCIRC,1992). In contrast to these daily spatial and temporal excursions of the tides, storm surge hydrograph durations last only for hours or for a few days before average daily tidal conditions are restored. The spatial surface area is increased as the flooded areas are included in the numerical model simulations of storm surge. When a "significant" coastal storm occurs, the movable tidal-flow gates are closed to prevent the storm surge from upland inundation and flood damage. The gates are reopened when storm surge levels return to near normal tidal conditions. The connection to the ocean permits elevated water levels from storm events to penetrate inland causing inundation and flood damage. And that is the problem which will only get worse in the future.

The barrier at the entrance to a tidal estuary must also cross existing navigation channels connecting to inland ports and marinas (see Figure 1). Water depths in the channels may be natural or deepened by dredging to permit deep-draft vessels to access the port. The movable tidal-flow gates at the navigation channel must allow ships to freely pass the barrier when open, but also must be of sufficient depth to block storm surge flows from passing beneath the gate when closed. These restrictions generally prohibit the location of tidal-flow turbines within the deepened navigation channel.

Summary of Constructed Storm Surge Barriers (1958-2020)

There are six different types of movable, tidal-flow and navigation-channel gates for storm surge barriers. Movement to close and open the gates is possible in the vertical and/or horizontal directions. The vertical lift gate shown in Figure 7 (upper middle) for the famous Eastern Scheldt SSB in the Netherlands is moved upward by hoisting cables or hydraulic pressure cylinders for ease of inspection and maintenance but prohibits its use in the navigation channel for ship passage. However, tidal-flows through open gates readily permit tidal-turbines to be installed immediately adjacent to the opening and the superstructure can convey the power generation cables.

Two gate types (miter and sector gates) rotate horizontally and are now routinely employed for closure in locks and navigation channels, respectively since they cause no obstruction for ships. The remaining three types (flap, vertical rotating, and inflatable rubber) lay on the bottom of the channel to also pose no obstruction for ships passing the barrier. See Dircke et al. 2012 and Hillen et al. 2010 for illustrations of all six types and Figure 7 for photos with locations as examples. All the above six types of movable tidal flood gates have been constructed and are currently functioning in storm surge barriers in Western Europe and the United States. There is no one "best" type. Site specific conditions, economics and the future of tribrid functional design-criteria will govern their selection.

Figure 7 Example of the six types of movable, tidal-flow and navigation-channel gates for storm surge barriers.

A summary of the existing 19 storm surge barriers may help with a preliminary design with the key physical dimensions presented in Table I (adapted from Mooyaart et al. 2014). Barrier lengths range from 40m (Hull, UK) to 9000m (Eastern Scheldt, Holland). The one exception of over 25,400m is in Russia (St. Petersburg) where the length is due to its function as the last completed section of a ring road. It includes a tunnel beneath the navigation channel to insure continuous passage for vehicles.

The in-water, movable gate span width and number give the gate opening width for the ecology function. They all may have the same span width with four shown in Figure 1. For navigation, a horizontal, sector gate of opening width is shown in Figure 7 (bottom left). There may be more than one navigation channel crossing the tidal barrier. A third possible opening is through a lock for ship passage past the barrier that is only needed when all the other gates are closed (none shown in Figure 1). The combined total opening width, $W_T = W_E + W_N + W_L$. The total barrier length, L_B includes the lengths of flood walls and housing for all the mechanical and electrical equipment to operate the gates.

Table I Storm surge barriers in Western Europe and USA,1958-2020 (adapted from Mooyaart et al (2014)

Storm Surge Barriers					Ecology Gated Width We (m)	Navigation Gated Width Wn (m)	Lock Flood Gates Closed, Wl (m)	Combined Total Opening Wt= We+Wn+Wl (m)	Percent Opening Wt/Lв	Cost per meter (2014) M(€)/m
Number	Chronological Order Name	Constructed (1958- to date) Location (Country)	Dates	Total Barrier Length,Lв (m)						
1	Hollandsche Ijssel	Krimpen (Netherlands)	1954-1958	200		80	24	104	52.0	2.16
2	Fox Point	Providence, RI (USA)	1961-1966	915		36.6		36.6	4.0	
3	New Bedford	New Bedford, MA (USA)	1962-1966	1370		46		46	3.4	2.65
4	Billwerder Bucht	Hamburg (Germany)	1964-1966	150	60	68		128	85.3	
5	Stamford	Stamford, CT (USA)	1965-1969	870		27		27	3.1	3.07
6	Eider	Tonning (Germany)	1967-1973	4900	200		14	214	4.4	1.38
7	Hull	Hull (United Kingdom)	1977-1980	40		30		30	75.0	0.63
8	Thames	London (UK)	1974-1982	530	124	307		431	81.3	3.88
9	Eastern Scheldt	Scheldt (Netherlands)	1973-1986	9000	2604		16	2620	29.1	1.76
10	Maeslant	Rotterdam (Netherlands)	1989-1997	610		360		360	59.0	1.86
11	Hartel	Spijkenisse (Netherlands)	1993-1997	250		147	15	162	64.8	0.99
12	Ramspol	Ens (Netherlands)	1996-2002	450	150	75		225	50.0	0.67
13	Ems	Gamdersum (Germany)	1998-2002	476	264	110		374	78.6	1.03
14	St. Petersburg	St. Petersburg (Russia)	1955-2011	25400	1536	310		1846	7.3	3.56
15	IHNC (Lake Borgne)	New Orleans (USA)	2008-2011	2300		107		107	4.7	3.97
16	Seabrook	New Orleans (USA)	2008-2011	130	30	29		59	45.4	2.15
17	Harvey Canal	New Orleans (USA)	2008-2011	120		38		38	31.7	
18	West Closure-GIWW	Southeast LA (USA)	2008-2012	525		69		69	13.1	
19	MOSE	Venice (Italy)	2003-2020	1600	400	1180		1580	98.8	3.20

Clearly, navigation is the most important function for a barrier opening since seventeen (89%) required a gated section for navigation. Nine barriers (47%) included movable-gates for tidal-flows to enhance the ecological needs of the tidal estuary. Only three (16%) included a lock section for ship passage when the barrier gates were closed for a storm. None had all three types of gate openings. The combined total opening is then listed in Table I along with the ratio as the percent of tidal-flow barrier opening relative to the barrier length. The average percent opening was 41.6%. However, USA percent openings averaged only 15.1% compared with Western Europe's 61.7%.

The impacts of numerous storm surge events on the tourism industry is the primary reason for a storm surge barrier as now operating for Venice in Italy. The MOSE project for Venice provides pneumatic flap gates for the three inlet openings to the Venice Lagoon for navigation but also includes a movable-gated section that adds 23% to the total opening. The result is that the total percent opening is 98% of the barrier length and by far the most efficient from an ecological and environmental perspective. The three tidal inlets (Lido, Malamoco, and Chioggia,) that funnel storm surges from the Adriatic Sea into the Venice Lagoon and flood the City of Venice are shown in Figure 8 (upper left). Air-lift flap gates on a large concrete foundation are illustrated in the upper right and lower left schematics in Figure 8. This author visited the construction site at the Malamoco Inlet in 2013 with photo shown in Figure 8 (lower right). As of this writing, the **MOSE** (**MO**dulo **S**perimentale **E**lettromeccanico, *Experimental Electromechanical Module*) storm surge barrier project has passed a major first test of successful prevention of flooding in Venice on October 3, 2020 (Intl, NY Times, 2020).

Table I includes costs of fifteen constructed storm surge barriers in Western Europe and USA,1958-2017. Jonkman et al (2013) determined that costs for the movable-gate width, navigation width, and lock width when combined cost 10 to 100 times more than costs for the solid-wall section. Mooyaart et al. (2014) determined that total costs were more accurately predicted when the total opening width was employed (and not the barrier length) to determine cost per unit length. The results for the 15 constructed projects are listed in the last column in Table I in millions of Euros per meter, M (€/m) in the year 2014. The mean of these 15 projects was 2.2 M (€/m) with deviation of the mean, σ = 1.2 M (€/m) and a correlation coefficient equal 0.84 for a straight-line, linear fit of the data.

Hence, for early planning stages of a study of alternatives for construction costs, in millions of Euros per meter of length, M (€/m) for storm surge barriers use

$$C_{2014} = 2.2\, W_T \quad \text{with } \sigma = 1.2 \tag{5}$$

$W_T = $ total opening width in meters.

Aerts et al (2013) estimated that annual maintenance costs are 0.5 to 2 percent of the initial construction costs. Life-cycle costs must always be estimated for each alternative considered to mitigate damages from coastal flooding. Yearly cost indexes are available to bring the costs in year 2014 up to date.

The bottom line is that the storm surge barrier alternative with wide openings for minimal interference with daily tidal flows is expensive.

The data found in Table I has been compiled and checked from the following references: PIANC (2006), Morang (2007), Hillen et al. (2010), Hill, Bowman and Khinda, editors (2011), Dircke, Jongeling, and Jansen (2012), Jonkman et al. (2013), Mooyaart et al. (2014), Mooyaart and Jonkman (2017). For an update, see Mooyaart and Jonkman (2017) that includes an Appendix with photographs and many more details for most of the storm surge barriers listed in Table I
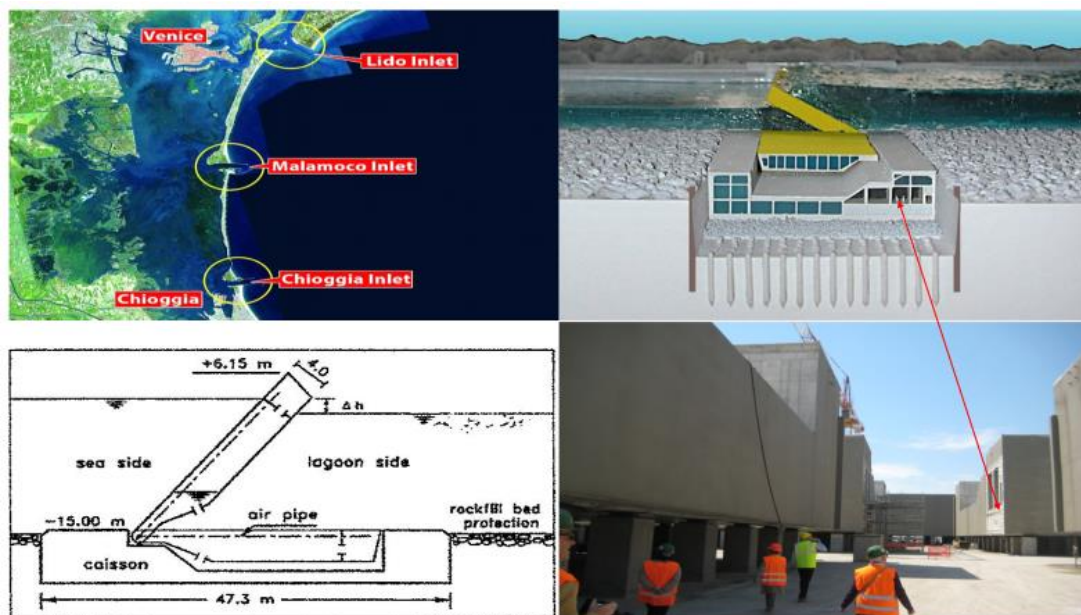

Figure 8 Location of inlets to Venice lagoon (upper, left), schematic of one foundation and air-lift gate (upper, right), schematic of the flap gate (lower, left) and photo during the authors visit to the Malamoco Inlet construction site in 2013 (lower, right).

Proposed New Projects

Recently proposed projects for storm surge barriers across the entrances to tidal inlets are illustrated in Figure 9.

(a) Boston Harbor. The University of Massachusetts, Boston, together with Arcadis Engineering and the Woods Hole Group made a feasibility study of harbor-wide barrier systems for Boston harbor (Sustainable Solutions Lab. 2018). Figure 9 (upper left) displays the Outer Harbor Barrier system location with two horizontal sector gates for the two navigation channels, the barrier wall sections (right side, green) and a number of "…*environmental flow control gates or openings in the barrier …that would be required for water quality…*" (right side, white dots). This report also states:

"*Future analysis would refine the number and net opening size required. There is some flexibility in the sizing and style of these* (gates)…"

9

Figure 9. Recent, proposed storm surge barrier designs for Boston Harbor (upper, left), NewYork/New Jersey Outer Harbor (upper right), Verrazano Bridge (lower left), and Houston/Galveston Bay (lower right)

(b) New York/ New Jersey Harbor.   The US Army, Corps of Engineers began work on the "New York-New Jersey Harbor and Tributaries Coastal Storm Risk Management Feasibility Study" (NYNJHAT) in 2016. A preliminary report was released in February, 2019 and included the study of many storm surge barrier locations as illustrated in Figure 9 (upper right).   The Outer Harbor barrier is 9900m (35,000 ft) long stretching from Sandy Hook, NJ to the tip at Breezy Point on Jamaica Bay. The barrier beneath the Verrazano Narrows bridge is 2135m (7000 ft) wide as shown in the section view, Figure 9 (lower left). Numerous tidal-flow gates are included in these designs as illustrated in Figure 9 (lower left) for vertical lift gates shown in the open position. The US Federal Government administration cancelled the final years of this study in January, 2020. Reasons for cancellation were not given.

(c) Texas- Galveston Bay/ Houston.   Figure 9 (lower right) is an aerial view of the proposed gate structures with separate, horizontal sector gates for the incoming and outgoing lanes of the Houston Ship Channel. The proposed storm surge barrier consists of two, 650 ft wide navigation channel gates; fifteen, 300 ft wide vertical lift gates for tidal flows; two 125 ft wide sector gates for recreation vessels (not shown); ninety-six, 16 ft wide, shallow water "environmental gates"; and the remaining barrier, a "Combi-wall" formed from vertical, cylinder piles with a concrete cap. The total length is 7200 ft (2.2 km). Mean tidal range is only 0.35m (1.16 ft).

 None of the feasibility studies for these three projects considered the generation of tidal-flow turbines located within the tidal-flow gates to generate electrical power.

Positive Impact SSB Under Future SLR

  Storm surge barriers designed for today's (2020) physical, environmental, and energy requirements, must also meet conditions possible in the years 2050 (30 yrs) and 2100 (80 yrs).

  Clearly, the most important variable is the crest elevation of the barrier. Water levels, water depths, and water wave conditions (heights, periods, directions) all impact wave setup, runup, and overtopping flowrates for a given crest elevation. The barrier slope, roughness and shape at the crest also are factors. Structure design that enables the crest elevation (or shape) to be economically altered (raised) in the future is desirable. For example, floating sector gates on the Maeslant (Holland) and St.

10

Petersburg (Russia) navigation channels are designed to float and remain a fixed distance above future sea levels at the site so that the wave runup and overtopping conditions remain relatively constant .

A second critical variable is the decision on when to close the gates. The time required and cost to close and then reopen the tidal-flow and navigation gates must be determined relative to the level of expected water levels and wave conditions during the storm. A storm surge barrier across a tidal inlet is never the total solution to mitigate storm damage. Climate change producing increasing sea levels will also increase the frequency and magnitude of all storm events so that who and how decisions are made requires input from many disciplines and the public. .

A third important variable is the choice of the dimensions of the gate to close the navigation channel. Tidal flow volumes through the deep channel(s) are the largest across the inlet; produce the majority of the storm surge elevation increase; and require most of the cost for the barrier. The width of the navigation gate opening can be less than the width of the navigation channel. For example, the navigation gate opening width of the Maeslant barrier is 360 m (Table I) while the Rotterdam Waterway width varies from 480 to 675 m wide. Ships passing simultaneously in opposite directions past the barrier may not be permitted.

Tidal energy is the only renewable energy resource that is available 24 hours each day over the entire year, with no downtime due to no sun or no wind or no waves. The daily tidal variation at the entrance to tidal estuaries is always present. Solar panels and wind turbine designs by themselves cannot be combined with flood damage mitigation structures.

SUMMARY

Design Goal No. 1 (Green Function)
In summary, under today's water levels, the goal is to minimize the loss of energy past the open gates to retain tidal wetlands at locations that exist today. This is accomplished using a large number of gates with large openings as for example, the Eastern Scheldt in Holland. Under future, much higher sea levels, the goal will be to maximize the energy loss past the open gates to retain the tidal wetlands that exist today.
Design the size and number of movable-gate openings in the storm surge barrier to produce an energy loss under future sea level rise conditions that will result in the future upstream limit of high tide water levels at or near the present-day location to maintain tidal wetlands.

Design Goal Number 2 (Blue Function)
Design the size and number of movable-gate openings in the storm surge barrier to accommodate the largest sizes and number of tidal-flow turbines installed at the gate openings to produce the greatest amount of electrical energy possible under future tidal-flow and sea level rise conditions.

Design Goal Number 3 (Grey Function)
Design the size and number of movable-gate openings and the navigation gate width in the storm surge barrier to be efficiently closed during storm surge conditions to reduce flood inundation and damage to all people and systems that are at risk under future sea level rise conditions.

It is clear that tradeoffs will be required to meet these three goals and that the costs of the barrier will also be an important factor.

The risk of flood damage in coastal areas of the world is increasing due to ever larger populations living in coastal regions and rising sea levels. Future design of storm surge barriers across tidal inlets with navigation gates and tidal-flow gates to reduce interior flood damage (when closed) and minimize ecological change (when open) are expensive. Daily high velocity tidal flows through the tidal-flow gate openings can drive tidal turbines to generate electricity. Money earned by tidal energy generation can be used to help pay for the high costs of storm surge barriers. All three functions of the barrier: storm damage mitigation (grey); maintenance of estuarine ecology (green); and renewable energy generation (blue) require tradeoffs in design. But when the grey, green, and blue functions are

combined, storm surge barriers will have a positive impact in the future of climate change where seas will be much higher and coastal storms more frequent and intense.

The world needs to replace fossil fuel energy sources with renewable energy resources to slow climate change and sea level rise.

REFERENCES

Basco, D.R. (2020) "*Combining Flood Damage Mitigation With Tidal Energy Generation: Lowering the Expense of Storm Surge Barrier Costs"*, 37th International Conference Coastal Engineering (ICCE), virtual conference, Oct 6-9.

Coastal Texas Study (2020) "*Study Overview*", US Army Corps of Engineers, Galveston District, Jan.

Corps of Engineers (2016) "*New York-New Jersey Harbor and Tributaries Coastal Storm Risk Management Feasibility Study*" (NYNJHAT), New York District, NY

Corps of Engineers (2018) "*Coastal Texas Protection and Restoration Feasibility Study*", Draft Integrated Feasibility Report and Environmental Impact Statement, Galveston District, October

Dewberry (2019) "*City-Wide Structural Alternatives for Coastal Flood Protection*", Interim Report for City of Virginia Beach, Dewberry Consulting Engineers, Alexandria, VA, May 24

Dircke, P.T.M., T.H.G. Jongeling, and P.L.M. Jansen (2012) "*Navigable Storm Surge Barriers for Coastal Cities: An Overview and Comparison"*, Climate Adaptation and Flood Risk in Coastal Cities, Earthscan, New York, NY, pp 201-223.

Dircke, P. T. M., T. H. G. Jongeling, and P. L. M. Jansen (2012) "*An Overview and Comparison of Navigable Storm Surge Barriers*", in Proceedings, Innovative Dam and Levee Design and Construction, USSD conference, New Orleans, LA, April.

GCCPRD, (2018) "*Phase 3 Report- Recommended Actions*", Gulf Coast Community Protection and Recovery District, Galveston, Texas

Hillen, M. M., S. N. Jonkman, W. Kanning, M. Kok, M. A. Geldenhuys, and M. J. F. Stive (2010) " *Coastal Defense Cost Estimates*" Delft Technical University, Comm. On Hydraulic and Geotechnical Engineering, April.

International NY Times (2020) "*Successful Test of Floodgates Leaves Venice Dry at High Tide*", Sunday, Oct 3.

Jonkman, S.N.; Hillen, M.M.; Nicholls, R.J.; Kanning, W., and van Ledden, M., 2013. "*Costs of adapting coastal defences to sea-level rise—new estimates and their implications".* Journal of Coastal Research, 29 (5), 1212 – 1226, Coconut Creek (Florida), ISSN 0749-0208.'

Khan, J. (2018) "*A Generic Performance Curve for Tidal and Hydrokinetic Devices*", Journal of Ocean Technology, vol 13, issue 2, pp 55-62)

Khojasteh, D., W. Glamore, V. Heimhuber, and S. Felder (2020) "*Sea Level Rise and Estuarine Tidal Dynamics: A review*" Earth-Science Reviews, March (Pre-proof).

Kilcher, L., R. Thresher and H. Tinnesand, (2016) "*Marine Hydrokinetic Energy Site Identification and Ranking Methodology Part II: Tidal Energy"*, Tech Rept. NREL/TP-5000-66079, National Renewable Energy Laboratory, Denver, October.

Luettich, R. A., J. J. Westerink, and N. W. Scheffner (1992), ADCIRC: An advanced three-dimensional circulation model for shelves, coasts, and estuaries. Report 1: Theory and methodology of ADCIRC-2DDI and ADCIRC-3DL, Dredging Res. Program Tech. Rep. DRP-92-6, Coastal Eng. Res. Cent., Vicksburg, Miss

Mooyaart, L.F., N.S. Jonkman, P.A.L.deVries, A. van der torn, and M. van Ledden (2014) "*Storm Surge Barrier: Overview and Design Considerations*", Proceedings, International Conference Coastal Engineering, ASCE, (Seoul).

Mooyaart, L.F. and S.N. Jonkman (2017) "*Overview and Design Considerations of Storm Surge Barriers*", Journal of Waterway, Port, Coastal and Ocean Engineering, ASCE, Vol 143 (July)

Morang, A. (2007) "*Hurricane Barriers in New England and New Jersey- History and Status After Four Decades*", Corps of Engineers, ERDC/CHL TR-07-11, September.

Sebastiaan N. Jonkman, Marten M. Hillen, Robert J. Nicholls, Wim Kanning, and Mathijs van Ledden (*2013) Costs of Adapting Coastal Defences to Sea-Level Rise— New Estimates and Their Implications*. Journal of Coastal Research: Volume 29, Issue 5: pp. 1212 – 1226.

Sustainable Solutions Lab (2018)."*Feasibility of Harbor-wide Barrier Systems: Preliminary Analysis for Boston Harbor*", Final Report, University of Massachusetts, Boston, May